

Barbie: Text to Barbie-Style 3D Avatars

Xiaokun Sun ¹, Zhenyu Zhang ^{1*}, Ying Tai ¹, Qian Wang ²,
 Hao Tang ³, Zili Yi ¹, Jian Yang ¹

¹Nanjing University ²China Mobile Research Institute ³Peking University
 xiaokun_sun@smail.nju.edu.cn, zhangjesse@foxmail.com, {yingtai, yi, csjyang}@nju.edu.cn,
 wangqianrg@chinamobile.com, bjdx tanghao@gmail.com

Abstract

Recent advances in text-guided 3D avatar generation have made substantial progress by distilling knowledge from diffusion models. Despite the plausible generated appearance, existing methods cannot achieve fine-grained disentanglement or high-fidelity modeling between inner body and outfit. In this paper, we propose Barbie, a novel framework for generating 3D avatars that can be dressed in diverse and high-quality Barbie-like garments and accessories. Instead of relying on a holistic model, Barbie achieves fine-grained disentanglement on avatars by semantic-aligned separated models for human body and outfits. These disentangled 3D representations are then optimized by different expert models to guarantee the domain-specific fidelity. To balance geometry diversity and reasonableness, we propose a series of losses for template-preserving and human-prior evolving. The final avatar is enhanced by unified texture refinement for superior texture consistency. Extensive experiments demonstrate that Barbie outperforms existing methods in both dressed human and outfit generation, supporting flexible apparel combination and animation. The code will be released for research purposes. Our project page is: <https://xiaokunsun.github.io/Barbie.github.io/>.

1 Introduction

In recent years, the creation of 3D digital humans has garnered significant attention due to its widespread applications in AR/VR. These applications yield the generated 3D avatars to have exquisite geometry, lifelike appearance, ultra-high diversity, and a faithful disentanglement of the human body and apparel. Usually, manually sculpting holistic 3D virtual humans is highly labor-intensive and time-consuming. Although progress (Ranjan et al. 2018; Ma et al. 2020; Chen et al. 2022) have been made on learning-based automatic human generation, these methods require large amounts of 3D human data for training, which greatly limits their application scope. Thanks to rapid progress on text-to-image (Rombach et al. 2022) and text-to-3D (Poole et al. 2022), leveraging natural language inputs for avatar generation has become increasingly popular recently.

The aforementioned text-to-avatar works can be roughly divided into two categories: generating (1) a holistic avatar and (2) disentangled models on body and apparel. Works on



Figure 1: Compared to holistic methods, Barbie effectively decouples the human body from different apparels while exhibiting fine details in the hands and head. In contrast to disentangled approaches, Barbie demonstrates a notable quality advantage and is capable of generating detailed accessories.

the former one (Hong et al. 2022; Kolotouros et al. 2024; Liao et al. 2024) are based on text-to-3D generation frameworks (Poole et al. 2022; Chen et al. 2023; Lin et al. 2023), and combined with human prior knowledge (Loper et al. 2015; Pavlakos et al. 2019; Alldieck, Xu, and Sminchisescu 2021) to improve the geometry fidelity of the generated results. Nevertheless, these works treat the human body, clothes, and accessories as a holistic model, which results in a loss of flexibility on applications such as virtual try-on and apparel transfer. As illustrated in Fig. 1-(a), these works cannot properly control garments and accessories with prompt. Consequently, a series of disentangled text-to-avatar works (Huang et al. 2023b; Wang et al. 2023a; Dong et al. 2024) have emerged. These methods employ multi-stage optimization strategies to model the body and clothes separately. However, these methods adopt a single general diffusion model to guide both body and garment generation, resulting in domain-specific fidelity loss on geometry or texture details. Furthermore, as illustrated in Fig. 1-(b), they fail to generate diverse and realistic outfits such as necklaces, glasses, hats, watches, or other accessories. The reason behind is two-fold: these methods lack of (1) fine-grained decomposition on avatar representation; (2) suitable constraints for optimization to generate in-domain components. In addition to this, generating fine-grained disentangled 3D avatars with realistic and text-aligned bodies, as well as garments and accessories, is still an open problem.

In this paper, we propose Barbie, a novel framework for generating Barbie-style 3D avatars that can be dressed in high-fidelity and diverse outfits, similar to the design of Bar-

*Corresponding author

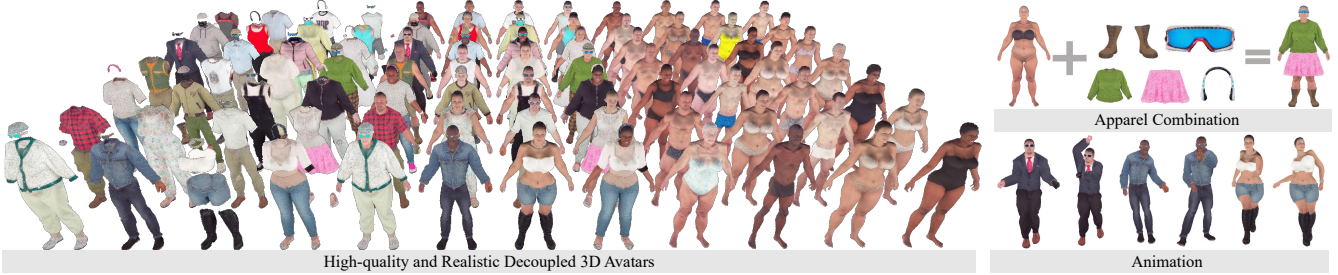


Figure 2: Using only texts as input, our method can generate Barbie-style 3D avatars. "Barbie-style" refers to (1) the generated 3D avatars exhibiting high quality and diversity; (2) the generated body, garments, and accessories being disentangled; and (3) the generated results supporting seamless apparel composition and user-friendly animation, similar to Barbie dolls.

bie dolls. As shown in Fig. 2, the avatars generated by Barbie have exquisite geometry and textures, and meanwhile wear various generated high-quality clothes and accessories that can be freely combined. Instead of generating bodies and all kinds of outfits guided by a single text-to-image (T2I) model, Barbie suitably involves different expert diffusion models to guarantee the domain-specific fidelity. Concretely, we first initialize different components of an avatar with semantic-aligned human prior to get disentangled representations. Then, each representation is optimized by corresponding expert T2I models to generate in-domain geometry and texture. During optimization, we propose human-prior evolving loss to enhance the diversity and description alignment for body generation, and template-preserving loss to suppress the artifacts of generated outfits. Finally, to balance the effect of different expert models, we propose an unified texture refinement to jointly optimize the composed avatar for more realistic appearance generation. In this way, the generated 3D avatars are disentangled and interactive with high-fidelity body, garments, and accessories, which is actually 'Barbie-style'.

Our main contributions are summarized as follows:

- We propose Barbie, a novel framework for creating realistic and highly disentangled 3D avatars in diverse body, garments, and accessories. To the best of our knowledge, Barbie should be the first work that achieves fine-grained text-to-avatar generation.
- We effectively employ expert models at different optimization stages to provide suitable guidance, boosting the generation quality on domain-specific realism. A series of novel losses and strategies are also proposed to address the geometry and texture conflicts when combining different expert models.
- Extensive experiments demonstrate that Barbie outperforms existing methods on avatar/outfit generation, showing superior geometry, texture, alignment on text description, and ability on fine-grained disentanglement.

2 Related Work

Text to 3D Content Generation. Motivated by the success of text-guided image generation, many works have focused on generating 3D content from textual prompts in a zero-shot manner. Early methods (Sanghi et al. 2022; Jain et al.

2022; Mohammad Khalid et al. 2022) use the CLIP model (Radford et al. 2021) to constrain the underlying 3D representations to align with the text descriptions. Nevertheless, the quality of created content is not satisfactory due to CLIP's limited generation capabilities. DreamFusion (Poole et al. 2022) then propose a score distillation sampling (SDS) loss, which enables more high-fidelity 3D content generation by utilizing a more powerful pre-trained T2I model (Rombach et al. 2022). Subsequently, a series of excellent works have emerged to boost the quality of text-to-3D generation through improvements on 3D representations (Chen et al. 2023; Yi et al. 2024), optimization strategies (Lin et al. 2023; Tang et al. 2023), SDS loss (Wang et al. 2024; Liang et al. 2024), and diffusion models (Li et al. 2023c; Qiu et al. 2024; Shi et al. 2023). However, these methods do not fully utilize the rich prior of the human body or generate realistic and high-quality 3D avatars.

Text to Holistic 3D Avatar Generation. AvatarCLIP (Hong et al. 2022) first realizes the zero-shot generation of 3D digital humans from text prompts by integrating human prior knowledge into Neus (Wang et al. 2021). With the introduction of SDS loss (Poole et al. 2022), many subsequent works (Jiang et al. 2023; Cao et al. 2024; Kolotouros et al. 2024; Mendiratta et al. 2023) combine it with parametric human models (Loper et al. 2015; Pavlakos et al. 2019; Alldieck, Xu, and Sminchisescu 2021), significantly improving the fidelity of the generated 3D digital humans. In addition, AvatarVerse (Zhang et al. 2024) and DreamWaltz (Huang et al. 2024b), inspired by ControlNet (Zhang, Rao, and Agrawala 2023), greatly enhance the 3D consistency of the generated results by adopting conditional diffusion models. TADA (Liao et al. 2024) and X-Oscar (Ma et al. 2024) propose using a subdivided SMPL-X model (Pavlakos et al. 2019) instead of implicit NeRF (Mildenhall et al. 2020) and Neus (Wang et al. 2021) to represent 3D digital humans. HumanNorm (Huang et al. 2024a) and SeeAvatar (Xu, Yang, and Yang 2023) achieve impressive geometric details by combining DMTet (Shen et al. 2021) with decoupled optimization strategies. Recently, HumanGaussian (Liu et al. 2024) and GAvatar (Yuan et al. 2024) introduced 3D Gaussian Splatting (Kerbl et al. 2023) to create fast-rendering high-quality 3D avatars. However, these approaches typically treat the human body, garments, and accessories as a holistic model, which loses the flexibility and controllability

of generation for further applications, such as the composition of clothing.

Text to Disentangled 3D Avatar Generation. To realize controllable avatar generation, a series of decoupled approaches have been proposed that separately model the human body and clothing through multi-stage optimization. HumanCoser (Wang et al. 2023b) and AvatarFusion (Huang et al. 2023b) using two radiation fields (Mildenhall et al. 2020; Wang et al. 2021) to represent the human body and all clothes, respectively. LAGA (Gong et al. 2024) and TELA (Dong et al. 2024) employ a layer-wise framework, representing each piece of clothing as an independent layer, further enhancing the flexibility and controllability of the generation. SO-SMPL (Wang et al. 2023a) replaces implicit representations (Mildenhall et al. 2020; Wang et al. 2021) with a more explicit SMPL-X (Pavlakos et al. 2019) representation. Nonetheless, these works employ a single general T2I model to guide both body and clothing generation, leading to a loss of geometry or texture fidelity in specific domains. Furthermore, they are unable to generate diverse and realistic outfits, such as necklaces, glasses, hats, watches, or other accessories.

In contrast to previous methods, the digital human generated by Barbie not only has fine geometry and realistic appearance but also wears multiple separable high-quality clothes and accessories. We summarize the main differences between our approach and related approaches in Fig. 1.

3 Methodology

3.1 Preliminaries

SMPL-X (Pavlakos et al. 2019) is a parametric human model that represents the full-body shape, pose, and expression using a small number of parameters. Given a set of shape parameters β , body pose parameters θ_{body} , jaw pose parameters θ_{face} , finger pose parameters θ_{hand} , and expression parameters ψ , it can generate a 3D human mesh M .

Score Distillation Sampling (Poole et al. 2022) leverages a pre-trained T2I model to guide the 3D representation to align with the input text. Given a text prompt y , a 3D representation with parameters θ , and a diffusion model with parameters ϕ , the SDS loss is defined as follows:

$$\nabla_{\theta} \mathcal{L}_{SDS} = \mathbb{E}_{t, \epsilon} \left[w(t) (\epsilon_{\phi}(x_t; y, t) - \epsilon) \frac{\partial x}{\partial \theta} \right], \quad (1)$$

where t is the time step in the 2D diffusion model, $x = g(\theta)$ is the image rendered from θ by a differentiable renderer g , $x_t = x + \epsilon$ is a noised version of x , $\epsilon_{\phi}(x_t; y, t)$ is the denoised image, and $w(t)$ is the weight function. For simplicity, we omit $w(t)$ in the following formulas.

DMTet (Shen et al. 2021) is a hybrid representation consisting of an implicit signed distance function (SDF) and a differentiable marching tetrahedra layer. The SDF can be efficiently represented by an MLP with multi-resolution hash encoding (Müller et al. 2022).

3.2 Overview

Given a prompt, Barbie aims to generate a disentangled 3D digital human dressed in high-fidelity and diverse garments

and accessories, similar to Barbie dolls. Fig. 3 shows the overview of the pipeline with three crucial stages. To guarantee the quality of generated body and outfits, we employ targeted expert diffusion models with specific regularization to produce a high-fidelity and reasonable human body (Sec. 3.3) and outfits (Sec. 3.4). The final composed avatar is jointly fine-tuned with unified texture refinement to achieve a more harmonious and consistent appearance (Sec. 3.5).

3.3 Human Body Generation

Human Body Initialization. Following HumanNorm and RichDreamer, we adopt DMTet as our 3D representation. Since DMTet is highly sensitive to initialization, we use SMPL-X mesh to build an accurate initial input. Concretely, we employ a differentiable renderer (Laine et al. 2020) and SDS loss to optimize the shape parameters β according to the input base human body description, thereby determining the basic body shape of the digital human. This initialized mesh M_{init} will be used in subsequent stages to provide rich human prior knowledge and ensure a semantic-aligned representation for the outfit.

Human Body Geometry Modeling. We then learn to optimize the initialized DMTet into disentangled geometry and texture. As discussed in introduction, using a single general T2I model struggles to provide domain-specific constraints for creating realistic human body or outfits. Therefore, we employ the human-specific diffusion models in HumanNorm (Huang et al. 2024a) which is fine-tuned on high-fidelity 3D human data for detailed body modeling.

In particular, human-specific diffusion models include a normal-adapted diffusion model ϕ_{hn} , a depth-adapted diffusion model ϕ_{hd} , as well as a normal-conditioned diffusion model ϕ_{hc} for human texture creation. ϕ_{hn} and ϕ_{hd} fully capture human geometry information and generate high-quality normal and depth images based on the input minimal-clothed human body description y_{h} . These models optimize the initialized human DMTet parameterized by θ_{h} with the following SDS loss:

$$\nabla_{\theta_{\text{h}}} \mathcal{L}_{SDS}^{\text{hn}} = \mathbb{E}_{t, \epsilon} \left[(\epsilon_{\phi_{\text{hn}}}(n_t^{\text{h}}; y_{\text{h}}, t) - \epsilon) \frac{\partial n^{\text{h}}}{\partial \theta_{\text{h}}} \right], \quad (2)$$

$$\nabla_{\theta_{\text{h}}} \mathcal{L}_{SDS}^{\text{hd}} = \mathbb{E}_{t, \epsilon} \left[(\epsilon_{\phi_{\text{hd}}}(d_t^{\text{h}}; y_{\text{h}}, t) - \epsilon) \frac{\partial d^{\text{h}}}{\partial \theta_{\text{h}}} \right], \quad (3)$$

where n^{h} and d^{h} are the rendered normal and depth maps of the human body, respectively.

Self-Evolving Human Prior Loss. Although Eqs. (2) and (3) leads to detailed human body generation, the overly strong generative prior of human-specific diffusion models may urge the generated results to overfit the input text, resulting in unnatural geometry and exaggerated body proportions. Introducing the constraints from parametric human models is an intuitive solution, but it loses the diversity and fine details. To solve this problem, we draw inspiration from SeeAvatar (Xu, Yang, and Yang 2023) and propose a self-evolving human prior loss. In particular, we periodically fit the initial mesh M_{init} to the generated DMTet, which is for-

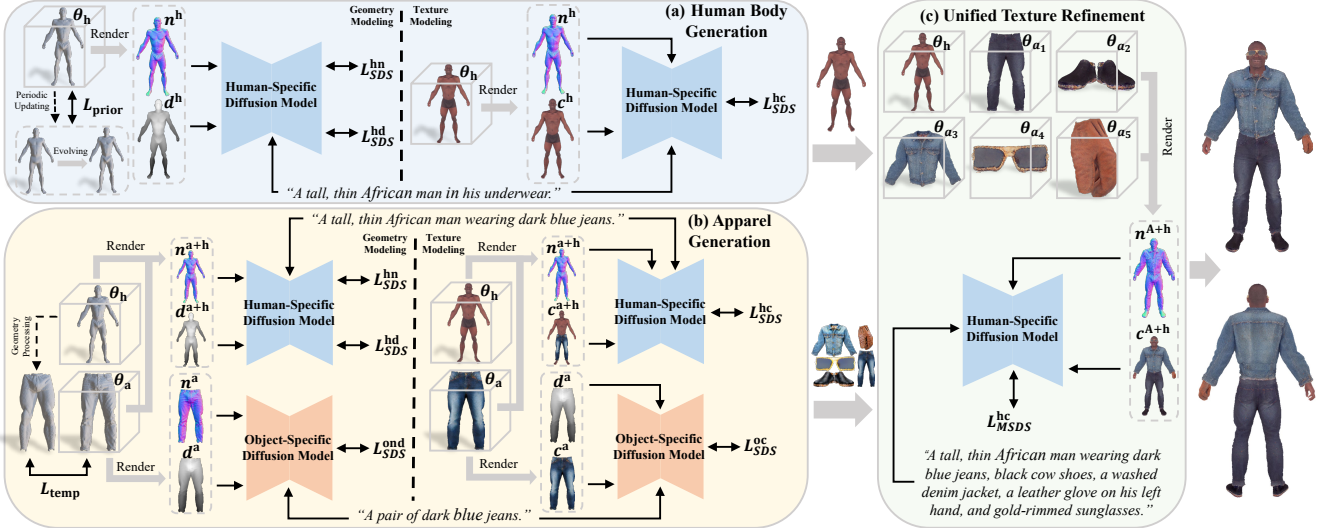


Figure 3: Barbie consists of three stages: (a) Using human-specific diffusion models and self-evolving human prior loss, Barbie generates a plausible and high-fidelity basic human body; (b) Initializing with the semantic-aligned template mesh, Barbie creates high-quality clothes and accessories piece by piece using object-specific diffusion models and template-preserving loss; (c) Finally, Barbie jointly fine-tunes the assembled avatar to further enhance the texture harmony and consistency.

mulated as:

$$\mathcal{L}_{\text{prior}} = \sum_{p \in P} \left\| s_{\theta_h}(p) - s_{\hat{M}_{\text{init}}}(p) \right\|_2^2, \quad (4)$$

where s_{θ_h} and $s_{\hat{M}_{\text{init}}}$ are the SDF functions of the generated body DMTet and the periodically evolved mesh from M_{init} , respectively. P is a set of randomly sampled points in space. s_{θ_h} is optimized every step, while $s_{\hat{M}_{\text{init}}}$ is optimized every 1000 steps. In this way, s_{θ_h} is regularized by the reliable human prior from \hat{M}_{init} , while \hat{M}_{init} is self-evolved to fit the current avatar geometry by learnable vertex displacements that represent geometric details. During the evolution process, \hat{M}_{init} gradually captures rich geometric features, such as muscle lines, providing reliable but diverse human priors for subsequent geometry creation. Compared with simply using SMPL-X SDF constraints, our self-evolving human prior loss enhances the limited parametric model, achieving a balance between diversity and rationality of geometry generation. In contrast to SeeAvatar, our loss retains the topological structure of SMPL-X, supporting the subsequent outfit initialization, composition, and animation.

In summary, the loss function for optimizing the human body geometry is as follows:

$$\mathcal{L}_{\text{hum-geo}} = \mathcal{L}_{SDS}^{hn} + \mathcal{L}_{SDS}^{hd} + \lambda_{\text{prior}} \mathcal{L}_{\text{prior}}. \quad (5)$$

Human Body Texture Modeling. Given the human mesh generated from the previous stage, we can create realistic and normal-aligned textures using ϕ_{hc} with loss as:

$$\nabla_{\theta_h} \mathcal{L}_{SDS}^{hc} = \mathbb{E}_{t, \epsilon} \left[(\epsilon_{\phi_{hc}}(c_t^h; n^h, y_h, t) - \epsilon) \frac{\partial c^h}{\partial \theta_h} \right], \quad (6)$$

where c^h represents the rendered color image of the generated human body. It's worth mentioning that experiments using Physically Based Rendering (PBR) lead to unnatural or

unrealistic appearances. Empirically, we adopt simple RGB rendering, and the experimental comparison are available in the supplementary material.

3.4 Apparel Generation

Apparel Initialization. With the body topology retained by our proposed self-evolving human prior loss, we can easily provide semantically aligned initialization for various apparel. Specifically, we utilize the human body segments of SMPL-X and pre-defined masked templates to cover more than a dozen types of daily clothing and accessories. By cropping the corresponding sub-mesh according to the apparel type, we obtain a closed template mesh M_{temp} to initialize the apparel DMTet through geometry processing such as scaling and sewing. For further details, please refer to the supplementary material.

Apparel Geometry Modeling. Similar to human body geometry generation, we utilize human-specific diffusion models to optimize outfit geometry with the following SDS loss:

$$\nabla_{\theta_a} \mathcal{L}_{SDS}^{hn} = \mathbb{E}_{t, \epsilon} \left[(\epsilon_{\phi_{hn}}(n_t^{a+h}; y_{a+h}, t) - \epsilon) \frac{\partial n^{a+h}}{\partial \theta_a} \right], \quad (7)$$

$$\nabla_{\theta_a} \mathcal{L}_{SDS}^{hd} = \mathbb{E}_{t, \epsilon} \left[(\epsilon_{\phi_{hd}}(d_t^{a+h}; y_{a+h}, t) - \epsilon) \frac{\partial d^{a+h}}{\partial \theta_a} \right], \quad (8)$$

where θ_a is the apparel DMTet parameters, y_{a+h} is the text description of the appereled avatar, and n^{a+h} and d^{a+h} are the rendered appereled human normal and depth maps, respectively. However, human-specific diffusion models are not well-suited for creating clothes and accessories, as they lack of in-domain details and diversity of generated outfits. Hence, we additionally introduce the object-specific diffusion models proposed by RichDreamer (Qiu et al. 2024),

which are trained on large-scale LAION dataset (Schuhmann et al. 2022).

Concretely, these diffusion models include a normal-depth diffusion model ϕ_{ond} for optimizing the apparel geometry, and a depth-conditional diffusion model ϕ_{oc} for creating the apparel texture. The normal-depth model provides effective supervision for outfit geometry generation by accurately modeling the joint distribution of normal and depth maps using the following SDS loss:

$$\begin{aligned} \nabla_{\theta_a} \mathcal{L}_{\text{SDS}}^{\text{ond}} &= \mathbb{E}_{t, \epsilon} \left[(\epsilon_{\phi_{\text{ond}}}(n_t^a; y_a, t) - \epsilon) \frac{\partial n^a}{\partial \theta_a} \right] \\ &+ \mathbb{E}_{t, \epsilon} \left[(\epsilon_{\phi_{\text{ond}}}(d_t^a; y_a, t) - \epsilon) \frac{\partial d^a}{\partial \theta_a} \right], \end{aligned} \quad (9)$$

where y_a is the text description of a single garment or accessory, and n^a and d^a are the rendered normal and depth maps of the apparel in the undressed state. In this way, the object-specific diffusion models provide a powerful geometry prior for generating high-fidelity clothes and accessories.

Template-Preserving Loss. Similar to human-specific diffusion models, relying on the object-specific diffusion models may lead to geometric artifacts such as holes (Sec. 4.4). To address this problem, we propose a template-preserving loss that enforces the apparel geometry to cover the template mesh M_{temp} during the optimization process to ensure geometric integrity. The loss function is formulated as follows:

$$\mathcal{L}_{\text{temp}} = \sum_{p \in P_{\text{temp}}} \max(0, s_{\theta_a}(p)), \quad (10)$$

where s_{θ_a} represents the SDF function of apparel DMTet and P_{temp} is the set of randomly sampled points inside the template mesh.

Specifically, this loss guarantees that the apparel geometry covers the template mesh by pushing the sampled SDF values of s_{θ_a} inside the template mesh to be negative. Instead of employing the MSE function to provide prior constraints such as Eq. (4), the template-preserving loss only restricts the SDF values of the points inside the template, ensuring geometric rationality without limiting the sculpting of geometric details outside the template mesh.

In summary, the loss function for optimizing the apparel geometry is as follows:

$$\mathcal{L}_{\text{app-geo}} = \mathcal{L}_{\text{SDS}}^{\text{hn}} + \mathcal{L}_{\text{SDS}}^{\text{hd}} + \mathcal{L}_{\text{SDS}}^{\text{ond}} + \mathcal{L}_{\text{SDS}}^{\text{sd}} + \lambda_{\text{temp}} \mathcal{L}_{\text{temp}}, \quad (11)$$

where $\mathcal{L}_{\text{SDS}}^{\text{sd}}$ is the vanilla Stable Diffusion (SD) SDS loss enforced on the rendered apparel normal maps. As shown in RichDreamer, native SD helps object-specific diffusion models produce more stable results.

Apparel Texture Modeling. Given the generated dress geometry and the textured human body, we employ an object-specific depth-conditional diffusion model for lifelike apparel textures with the following SDS loss:

$$\nabla_{\theta_a} \mathcal{L}_{\text{SDS}}^{\text{oc}} = \mathbb{E}_{t, \epsilon} \left[(\epsilon_{\phi_{\text{oc}}}(c_t^a; d_t^a, y_a, t) - \epsilon) \frac{\partial c^a}{\partial \theta_a} \right], \quad (12)$$

where c^a is apparel color image. Additionally, human-specific diffusion models are combined to optimize the appearance of outfits in the dressed state to ensure basic texture

harmony, and the SDS loss is formulated as:

$$\nabla_{\theta_a} \mathcal{L}_{\text{SDS}}^{\text{hc}} = \mathbb{E}_{t, \epsilon} \left[(\epsilon_{\phi_{\text{hc}}}(c_t^{\text{a+h}}; n^{\text{a+h}}, y_{\text{a+h}}, t) - \epsilon) \frac{\partial c^{\text{a+h}}}{\partial \theta_a} \right]. \quad (13)$$

In summary, the loss function for optimizing the apparel appearance is as follows:

$$\mathcal{L}_{\text{app-tex}} = \mathcal{L}_{\text{SDS}}^{\text{hc}} + \mathcal{L}_{\text{SDS}}^{\text{oc}} + \mathcal{L}_{\text{SDS}}^{\text{sd}}. \quad (14)$$

3.5 Unified Texture Refinement

With the stage of human body and apparel generation, we produce human bodies, garments, and accessories with delicate geometry and plausible textures. However, the large domain gap between the training data used to fine-tune different expert models leads to texture incongruity between the human body and outfits, which significantly impacts the overall realism of the generated digital human (Sec. 4.4).

To address this challenge, we propose a unified texture refinement (UTR) strategy, which jointly fine-tunes the appearance of the assembled avatar under the multi-step SDS (MSDS) proposed by HumanNorm (Huang et al. 2024a). The loss function for UTR is formulated as follows:

$$\nabla_{\theta_A} \mathcal{L}_{\text{MSDS}}^{\text{hc}} = \mathbb{E}_{t, \epsilon} \left[(H(c_t^{\text{A+h}}; n^{\text{A+h}}, y_{\text{A+h}}, t) - \epsilon) \frac{\partial c^{\text{A+h}}}{\partial \theta_A} \right], \quad (15)$$

where H denotes the multi-step operation function (see HumanNorm for more details), $\theta_A = \{\theta_{a_i}, i \in [1, \dots, N]\}$ refers to the parameters of all apparel DMTets, $y_{\text{A+h}}$ is the full text description of the avatar wearing all outfits, and $n^{\text{A+h}}$ and $c^{\text{A+h}}$ are the rendered normal and color images of the avatar wearing all clothes and accessories. Unlike Eq. (14), we only use the human-specific normal-conditioned diffusion model to ensure overall texture style unity. Besides, we use the MSDS loss instead of the native SDS loss to further enhance texture realism, leading to more natural textures. In this way, UTR enhances the texture harmony and consistency of the generated avatar.

3.6 Implementation Details

Our algorithm is implemented using PyTorch (Paszke et al. 2019) and ThreeStudio (Guo et al. 2023). All experiments are conducted on an Ubuntu server equipped with A6000 GPUs. Generating a human body takes roughly 3 hours with 24GB memory, and generating a cloth or accessory takes roughly 4 hours with 40GB memory. Given a text describing an appareled human, e.g., "A man wearing X1 and X2", we first generate a base human body based on "A man in his underwear". We then generate the apparel X1 based on "A piece of X1" and "A man wearing X1", and then generate the apparel X2 based on "A piece of X2" and "A man wearing X1 and X2". Finally, fine-tune the overall texture based on the full input text "A man wearing X1 and X2". Additional details can be found in supplementary materials.

4 Experiments

4.1 Experimental Settings

Due to space limitations, we present only the most important experimental settings and results here. For complete results



Figure 4: Diverse Range of Barbie-Style Avatar Generation. Rendering color images and normal images for visualization. Please zoom in to see the details. See supplementary materials for video results.

Method	B-VQA \uparrow	B2-VQA \uparrow	GQP \uparrow	TAP \uparrow
DreamWaltz	0.5819	<u>0.5333</u>	5.67	6.67
TADA	0.5306	<u>0.5333</u>	6.33	6.67
X-Oscar	0.5069	0.5292	7.33	2.67
HumanGaussian	<u>0.6222</u>	0.5069	7.00	4.67
HumanNorm	0.5611	0.5292	7.67	6.67
Barbie (Ours)	0.7514	0.5778	66.00	72.67
DreamFusion	0.6633	0.5367	3.33	3.00
Fantasia3D	0.6750	0.4633	0.33	0.33
MVDream	0.7000	0.5933	<u>17.33</u>	<u>15.67</u>
GaussianDreamer	0.7017	0.5283	8.33	11.67
RichDreamer	0.8100	<u>0.6667</u>	6.33	7.33
Barbie (Ours)	0.7917	0.6933	64.33	62.00

Table 1: Quantitative comparisons with the SOTA methods. The best and second-best results are highlighted in bolded and underlined, respectively. B-VQA: BLIP-VQA. B2-VQA: BLIP2-VQA. GQP: generation quality preference (%), TAP: text-image alignment preference (%).

and details, please refer to our supplementary materials.

Baselines. We compare Barbie with the state-of-the-art (SOTA) methods for dressed avatar generation and apparel generation. The compared text-to-avatar methods include DreamWaltz (Huang et al. 2024b), TADA (Liao et al. 2024), X-Oscar (Ma et al. 2024), HumanGaussian (Liu et al. 2024), and HumanNorm (Huang et al. 2024a). The compared text-to-object methods include DreamFusion (Poole et al. 2022), Fantasia3D (Chen et al. 2023), MVDream (Shi et al. 2023), GaussianDreamer (Yi et al. 2024), and RichDreamer (Qiu et al. 2024). Additionally, we provide a qualitative comparison with the latest generation work that has not yet published code in the supplementary material.

Dataset Construction. We utilized ChatGPT to randomly generate 30 text descriptions of appareled avatars, with each example wearing a top, a bottom, a pair of shoes, and two random accessories. 30 descriptions for dressed humans are used to evaluate avatar generation, and 30×5 apparel descriptions are used to evaluate apparel generation. The com-

plete descriptions are listed in the Appendix.

Evaluation Metrics. Existing text-to-3D approaches utilize CLIP-based metrics to evaluate text-image alignment and compare the quality of generated results. However, CLIP-based metrics have been shown (Huang et al. 2023a; Lu et al. 2024) to be insufficient to accurately measure the fine-grained correspondence between 3D content and input prompts, which is further confirmed by experiments in the supplementary material.

Consequently, inspired by Progressive3D (Cheng et al. 2023), we adopt fine-grained text-to-image evaluation metrics including BLIP-VQA (Li et al. 2022, 2023a) and BLIP2-VQA (Li et al. 2023b,a) to evaluate the generation capacity of current methods and Barbie. Specifically, we first convert the prompt into multiple separate questions to retrieve corresponding content, then feed the rendered image of the 3D generated content into the VQA model and ask questions one by one, and finally use the probability of answering “yes” as the evaluation metric. For instance, the input avatar prompt “A man wearing X1.” is converted into “Is the person in the picture a man?” and “Is the person in the picture wearing X1?”. The input apparel prompt “A pair of X1.” is converted into “Is the object in the picture a pair of X1?”. Finally, we randomly select 10 examples from the generated results to conduct a user study and ask 30 volunteers to assess (1) generation quality and (2) text-image alignment, and select the preferred methods.

4.2 Comparisons of Dressed Avatar Generation

As shown in the upper part of Tab. 1, our method significantly outperforms the comparison methods across all metrics. The qualitative comparisons illustrated in the upper part of Fig. 5 further highlight the strength of our approach. Compared to other methods, the digital humans generated by Barbie exhibit finer and plausible geometric details, and ensure higher alignment with the input text without omitting any clothing or accessories. Additionally, unlike other compared methods, Barbie’s generation process is flexible and controllable, and the generated bodies, clothes, and accessories can be freely combined.

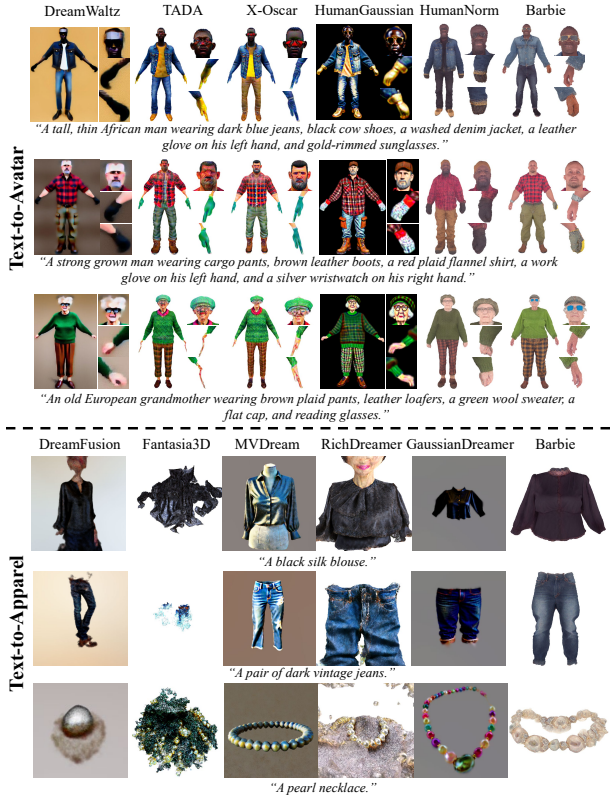


Figure 5: Qualitative comparisons with the SOTA methods.

4.3 Comparisons of Apparel Generation

As shown in the lower part of Tab. 1, our approach outperforms other methods on most evaluation metrics and is only slightly lower than RichDreamer (the SOTA open-source text-to-3D method) on BLIP-VQA, ranking the second. The qualitative comparisons illustrated in the lower part of Fig. 5 visualize some generation results. Compared to other methods, the clothes and accessories generated by Barbie exhibit more high-fidelity geometry and textures while maintaining high alignment with the text without incorporating incorrect content such as parts of the human body.

4.4 Ablation Study

Effect of Self-Evolving Human Prior Loss. As shown in Fig. 6-(a), omitting $\mathcal{L}_{\text{prior}}$ results in exaggerated human proportions, greatly reducing the realism of the generated results. Non-evolving human prior loss ensures the rationality of the generated human body, but it leads to over-smooth geometry or limited details. Using the full $\mathcal{L}_{\text{prior}}$ achieves both detailed and reasonable human body geometry generation.

Effect of Template-Preserving Loss. As shown in Fig. 6-(b), the template-preserving loss is crucial for ensuring the integrity of dress geometry. Omitting $\mathcal{L}_{\text{temp}}$ can result in holes or other geometry artifacts, significantly reducing the quality of the generated apparel.

Effect of Object-Specific Diffusion Models. Fig. 6-(c) shows that introducing an object-specific diffusion model

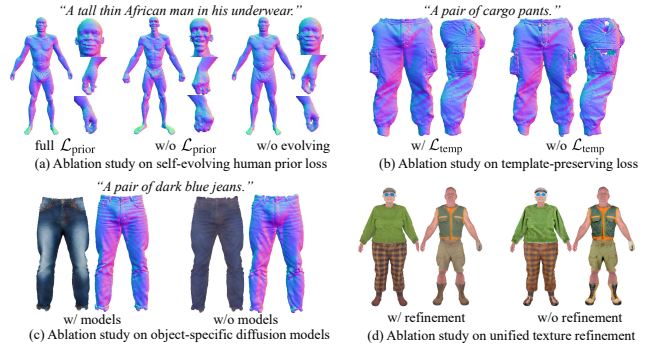


Figure 6: Ablation study on (a) self-evolving human prior loss, (b) template-preserving loss, (c) object-specific diffusion models supervision, and (d) unified texture refinement.



Figure 7: Applications of Barbie.

provides powerful guidance for creating finer geometric details and more lifelike appearance.

Effect of Unified Texture Refinement. Fig. 6-(d) demonstrates that UTR alleviates texture conflict between the human body and outfits. In addition, we also use the VQA model for quantitative comparison. Specifically, BLIP and BLIP2 have **98.33%** and **96.67%** probability of considering that the results after UTR have a more harmonious texture, which further proves that UTR greatly enhances the realism and consistency of the overall appearance.

4.5 Applications

As shown in Fig. 7-(a), our approach supports the free combination of any human body, garments and accessories, just like dressing Barbie dolls, which greatly improves the playability and reusability of text-to-avatar. With the self-evolving human prior loss, we can obtain an accurate correspondence between the generated human body and the SMPL-X model, allowing us to utilize the LBS algorithm to animate the generated avatars, as shown in Fig. 7-(b).

5 Conclusion

We propose Barbie, a novel method for creating Barbie-style 3D avatars which are dressed in disentangled, detailed, and diverse garments/accessories. To guarantee the domain-specific fidelity of the generated human body and outfits, we suitably combine different specific expert T2I models for domain-specific knowledge. To address the negative impacts caused by the over-strong generative priors of the expert models, we propose a series of well-designed loss functions and optimization strategies to ensure geometric rationality and texture harmony of the generated results. Extent-

sive experiments demonstrate that our approach outperforms the SOTA methods in both dressed avatar and apparel generation tasks.

References

Alldieck, T.; Xu, H.; and Sminchisescu, C. 2021. imghum: Implicit generative models of 3d human shape and articulated pose. In *Int. Conf. Comput. Vis.*, 5461–5470.

Cao, Y.; Cao, Y.-P.; Han, K.; Shan, Y.; and Wong, K.-Y. K. 2024. Dreamavatar: Text-and-shape guided 3d human avatar generation via diffusion models. In *IEEE Conf. Comput. Vis. Pattern Recog.*, 958–968.

Chen, R.; Chen, Y.; Jiao, N.; and Jia, K. 2023. Fantasia3d: Disentangling geometry and appearance for high-quality text-to-3d content creation. In *Int. Conf. Comput. Vis.*, 22246–22256.

Chen, X.; Jiang, T.; Song, J.; Yang, J.; Black, M. J.; Geiger, A.; and Hilliges, O. 2022. gdna: Towards generative detailed neural avatars. In *IEEE Conf. Comput. Vis. Pattern Recog.*, 20427–20437.

Cheng, X.; Yang, T.; Wang, J.; Li, Y.; Zhang, L.; Zhang, J.; and Yuan, L. 2023. Progressive3D: Progressively Local Editing for Text-to-3D Content Creation with Complex Semantic Prompts. In *Int. Conf. Learn. Represent.*

Dong, J.; Fang, Q.; Huang, Z.; Xu, X.; Wang, J.; Peng, S.; and Dai, B. 2024. TELA: Text to Layer-wise 3D Clothed Human Generation. *arXiv preprint arXiv:2404.16748*.

Gong, J.; Ji, S.; Foo, L. G.; Chen, K.; Rahmani, H.; and Liu, J. 2024. LAGA: Layered 3D Avatar Generation and Customization via Gaussian Splatting. *arXiv preprint arXiv:2405.12663*.

Guo, Y.-C.; Liu, Y.-T.; Shao, R.; Laforte, C.; Voleti, V.; Luo, G.; Chen, C.-H.; Zou, Z.-X.; Wang, C.; Cao, Y.-P.; and Zhang, S.-H. 2023. threestudio: A unified framework for 3D content generation. <https://github.com/threestudio-project/threestudio>.

Hong, F.; Zhang, M.; Pan, L.; Cai, Z.; Yang, L.; and Liu, Z. 2022. AvatarCLIP: zero-shot text-driven generation and animation of 3D avatars. *ACM Trans. Graph.*, 41(4): 1–19.

Huang, K.; Sun, K.; Xie, E.; Li, Z.; and Liu, X. 2023a. T2i-compbench: A comprehensive benchmark for open-world compositional text-to-image generation. *Adv. Neural Inform. Process. Syst.*, 36: 78723–78747.

Huang, S.; Yang, Z.; Li, L.; Yang, Y.; and Jia, J. 2023b. AvatarFusion: Zero-shot Generation of Clothing-Decoupled 3D Avatars Using 2D Diffusion. In *ACM Int. Conf. Multimedia*, 5734–5745.

Huang, X.; Shao, R.; Zhang, Q.; Zhang, H.; Feng, Y.; Liu, Y.; and Wang, Q. 2024a. Humannorm: Learning normal diffusion model for high-quality and realistic 3d human generation. In *IEEE Conf. Comput. Vis. Pattern Recog.*, 4568–4577.

Huang, Y.; Wang, J.; Zeng, A.; Cao, H.; Qi, X.; Shi, Y.; Zha, Z.-J.; and Zhang, L. 2024b. Dreamwaltz: Make a scene with complex 3d animatable avatars. *Advances in Neural Information Processing Systems*, 36.

Jain, A.; Mildenhall, B.; Barron, J. T.; Abbeel, P.; and Poole, B. 2022. Zero-shot text-guided object generation with dream fields. In *IEEE Conf. Comput. Vis. Pattern Recog.*, 867–876.

Jiang, R.; Wang, C.; Zhang, J.; Chai, M.; He, M.; Chen, D.; and Liao, J. 2023. Avatarcraft: Transforming text into neural human avatars with parameterized shape and pose control. In *Int. Conf. Comput. Vis.*, 14371–14382.

Kerbl, B.; Kopanas, G.; Leimkühler, T.; and Drettakis, G. 2023. 3d gaussian splatting for real-time radiance field rendering. *ACM Trans. Graph.*, 42(4): 1–14.

Kolotouros, N.; Alldieck, T.; Zanfir, A.; Bazavan, E.; Fieraru, M.; and Sminchisescu, C. 2024. Dreamhuman: Animatable 3d avatars from text. *Adv. Neural Inform. Process. Syst.*, 36.

Laine, S.; Hellsten, J.; Karras, T.; Seol, Y.; Lehtinen, J.; and Aila, T. 2020. Modular primitives for high-performance differentiable rendering. *ACM Trans. Graph.*, 39(6): 1–14.

Li, D.; Li, J.; Le, H.; Wang, G.; Savarese, S.; and Hoi, S. C. 2023a. LAVIS: A One-stop Library for Language-Vision Intelligence. In *Proceedings of the 61st Annual Meeting of the Association for Computational Linguistics (Volume 3: System Demonstrations)*, 31–41.

Li, J.; Li, D.; Savarese, S.; and Hoi, S. 2023b. Blip-2: Bootstrapping language-image pre-training with frozen image encoders and large language models. In *International Conference on Machine Learning*, 19730–19742.

Li, J.; Li, D.; Xiong, C.; and Hoi, S. 2022. Blip: Bootstrapping language-image pre-training for unified vision-language understanding and generation. In *International Conference on Machine Learning*, 12888–12900.

Li, W.; Chen, R.; Chen, X.; and Tan, P. 2023c. Sweet-Dreamer: Aligning Geometric Priors in 2D diffusion for Consistent Text-to-3D. In *Int. Conf. Learn. Represent.*

Liang, Y.; Yang, X.; Lin, J.; Li, H.; Xu, X.; and Chen, Y. 2024. Luciddreamer: Towards high-fidelity text-to-3d generation via interval score matching. In *IEEE Conf. Comput. Vis. Pattern Recog.*, 6517–6526.

Liao, T.; Yi, H.; Xiu, Y.; Tang, J.; Huang, Y.; Thies, J.; and Black, M. J. 2024. TADA! Text to Animatable Digital Avatars. In *International Conference on 3D Vision*.

Lin, C.-H.; Gao, J.; Tang, L.; Takikawa, T.; Zeng, X.; Huang, X.; Kreis, K.; Fidler, S.; Liu, M.-Y.; and Lin, T.-Y. 2023. Magic3d: High-resolution text-to-3d content creation. In *IEEE Conf. Comput. Vis. Pattern Recog.*, 300–309.

Liu, X.; Zhan, X.; Tang, J.; Shan, Y.; Zeng, G.; Lin, D.; Liu, X.; and Liu, Z. 2024. Humangaussian: Text-driven 3d human generation with gaussian splatting. In *IEEE Conf. Comput. Vis. Pattern Recog.*, 6646–6657.

Loper, M.; Mahmood, N.; Romero, J.; Pons-Moll, G.; and Black, M. J. 2015. SMPL: a skinned multi-person linear model. *ACM Trans. Graph.*, 34(6): 1–16.

Lu, Y.; Yang, X.; Li, X.; Wang, X. E.; and Wang, W. Y. 2024. Llmscore: Unveiling the power of large language models in text-to-image synthesis evaluation. *Adv. Neural Inform. Process. Syst.*, 36.

Ma, Q.; Yang, J.; Ranjan, A.; Pujades, S.; Pons-Moll, G.; Tang, S.; and Black, M. J. 2020. Learning to dress 3d people in generative clothing. In *IEEE Conf. Comput. Vis. Pattern Recog.*, 6469–6478.

Ma, Y.; Lin, Z.; Ji, J.; Fan, Y.; Sun, X.; and Ji, R. 2024. X-Oscar: A Progressive Framework for High-quality Text-guided 3D Animatable Avatar Generation. *arXiv preprint arXiv:2405.00954*.

Mendiratta, M.; Pan, X.; Elgharib, M.; Teotia, K.; Tewari, A.; Golyanik, V.; Kortylewski, A.; Theobalt, C.; et al. 2023. Avatarstudio: Text-driven editing of 3d dynamic human head avatars. *arXiv preprint arXiv:2306.00547*.

Mildenhall, B.; Srinivasan, P. P.; Tancik, M.; Barron, J. T.; Ramamoorthi, R.; and Ng, R. 2020. NeRF: Representing Scenes as Neural Radiance Fields for View Synthesis. In *Eur. Conf. Comput. Vis.*

Mohammad Khalid, N.; Xie, T.; Belilovsky, E.; and Popa, T. 2022. Clip-mesh: Generating textured meshes from text using pretrained image-text models. In *ACM SIGGRAPH Asia*, 1–8.

Müller, T.; Evans, A.; Schied, C.; and Keller, A. 2022. Instant neural graphics primitives with a multiresolution hash encoding. *ACM Trans. Graph.*, 41(4): 1–15.

Paszke, A.; Gross, S.; Massa, F.; Lerer, A.; Bradbury, J.; Chanan, G.; Killeen, T.; Lin, Z.; Gimelshein, N.; Antiga, L.; et al. 2019. Pytorch: An imperative style, high-performance deep learning library. *Advances in neural information processing systems*, 32.

Pavlakos, G.; Choutas, V.; Ghorbani, N.; Bolckart, T.; Osman, A. A.; Tzionas, D.; and Black, M. J. 2019. Expressive body capture: 3d hands, face, and body from a single image. In *IEEE Conf. Comput. Vis. Pattern Recog.*, 10975–10985.

Poole, B.; Jain, A.; Barron, J. T.; and Mildenhall, B. 2022. DreamFusion: Text-to-3D using 2D Diffusion. In *Int. Conf. Learn. Represent.*

Qiu, L.; Chen, G.; Gu, X.; Zuo, Q.; Xu, M.; Wu, Y.; Yuan, W.; Dong, Z.; Bo, L.; and Han, X. 2024. Richdreamer: A generalizable normal-depth diffusion model for detail richness in text-to-3d. In *IEEE Conf. Comput. Vis. Pattern Recog.*, 9914–9925.

Radford, A.; Kim, J. W.; Hallacy, C.; Ramesh, A.; Goh, G.; Agarwal, S.; Sastry, G.; Askell, A.; Mishkin, P.; Clark, J.; et al. 2021. Learning transferable visual models from natural language supervision. In *International Conference on Machine Learning*, 8748–8763.

Ranjan, A.; Bolckart, T.; Sanyal, S.; and Black, M. J. 2018. Generating 3D faces using convolutional mesh autoencoders. In *Eur. Conf. Comput. Vis.*, 704–720.

Rombach, R.; Blattmann, A.; Lorenz, D.; Esser, P.; and Ommer, B. 2022. High-resolution image synthesis with latent diffusion models. In *IEEE Conf. Comput. Vis. Pattern Recog.*, 10684–10695.

Sanghi, A.; Chu, H.; Lambourne, J. G.; Wang, Y.; Cheng, C.-Y.; Fumero, M.; and Malekshan, K. R. 2022. Clip-forge: Towards zero-shot text-to-shape generation. In *IEEE Conf. Comput. Vis. Pattern Recog.*, 18603–18613.

Schuhmann, C.; Beaumont, R.; Vencu, R.; Gordon, C.; Wightman, R.; Cherti, M.; Coombes, T.; Katta, A.; Mullis, C.; Wortsman, M.; et al. 2022. Laion-5b: An open large-scale dataset for training next generation image-text models. *Adv. Neural Inform. Process. Syst.*, 35: 25278–25294.

Shen, T.; Gao, J.; Yin, K.; Liu, M.-Y.; and Fidler, S. 2021. Deep marching tetrahedra: a hybrid representation for high-resolution 3d shape synthesis. *Adv. Neural Inform. Process. Syst.*, 34: 6087–6101.

Shi, Y.; Wang, P.; Ye, J.; Mai, L.; Li, K.; and Yang, X. 2023. MVDream: Multi-view Diffusion for 3D Generation. In *Int. Conf. Learn. Represent.*

Tang, J.; Ren, J.; Zhou, H.; Liu, Z.; and Zeng, G. 2023. DreamGaussian: Generative Gaussian Splatting for Efficient 3D Content Creation. In *Int. Conf. Learn. Represent.*

Wang, J.; Liu, Y.; Dou, Z.; Yu, Z.; Liang, Y.; Li, X.; Wang, W.; Xie, R.; and Song, L. 2023a. Disentangled Clothed Avatar Generation from Text Descriptions. *arXiv preprint arXiv:2312.05295*.

Wang, P.; Liu, L.; Liu, Y.; Theobalt, C.; Komura, T.; and Wang, W. 2021. NeuS: Learning Neural Implicit Surfaces by Volume Rendering for Multi-view Reconstruction. *Adv. Neural Inform. Process. Syst.*, 34: 27171–27183.

Wang, Y.; Ma, J.; Shao, R.; Feng, Q.; Lai, Y.-K.; Liu, Y.; and Li, K. 2023b. HumanCoser: Layered 3D Human Generation via Semantic-Aware Diffusion Model. *arXiv preprint arXiv:2312.05804*.

Wang, Z.; Lu, C.; Wang, Y.; Bao, F.; Li, C.; Su, H.; and Zhu, J. 2024. Prolificdreamer: High-fidelity and diverse text-to-3d generation with variational score distillation. *Adv. Neural Inform. Process. Syst.*, 36.

Xu, Y.; Yang, Z.; and Yang, Y. 2023. SEEAvatar: Photorealistic Text-to-3D Avatar Generation with Constrained Geometry and Appearance. *arXiv preprint arXiv:2312.08889*.

Yi, T.; Fang, J.; Wang, J.; Wu, G.; Xie, L.; Zhang, X.; Liu, W.; Tian, Q.; and Wang, X. 2024. Gaussiandreamer: Fast generation from text to 3d gaussians by bridging 2d and 3d diffusion models. In *IEEE Conf. Comput. Vis. Pattern Recog.*, 6796–6807.

Yuan, Y.; Li, X.; Huang, Y.; De Mello, S.; Nagano, K.; Kautz, J.; and Iqbal, U. 2024. Gavatar: Animatable 3d gaussian avatars with implicit mesh learning. In *IEEE Conf. Comput. Vis. Pattern Recog.*, 896–905.

Zhang, H.; Chen, B.; Yang, H.; Qu, L.; Wang, X.; Chen, L.; Long, C.; Zhu, F.; Du, D.; and Zheng, M. 2024. Avatarverse: High-quality & stable 3d avatar creation from text and pose. In *AAAI*, volume 38, 7124–7132.

Zhang, L.; Rao, A.; and Agrawala, M. 2023. Adding conditional control to text-to-image diffusion models. In *Int. Conf. Comput. Vis.*, 3836–3847.